



# An analytical hierarchy process-based geospatial modeling for delineation of potential anthropogenic contamination zones of groundwater from Arang block of Raipur district, Chhattisgarh, Central India

Sudhakar Singha<sup>1</sup> · Srinivas Pasupuleti<sup>1</sup> · Krishna Sandilya Durbha<sup>2</sup> · Soumya S. Singha<sup>1</sup> · Rambabu Singh<sup>3</sup> · A. S. Venkatesh<sup>4</sup>

Received: 12 November 2018 / Accepted: 25 November 2019 / Published online: 4 December 2019  
© Springer-Verlag GmbH Germany, part of Springer Nature 2019

## Abstract

In the present study, identification of groundwater zones that are affected by anthropogenic contaminants based on litho-hydrogeological parameters has been attempted using multi-criteria decision analysis–analytical hierarchy process (MCDA–AHP) technique in an agriculturally intensive Arang block of Raipur district, Chhattisgarh, Central India. Litho-hydrogeological factors, such as geological and aquifer characteristics, land use–land cover, depth to water table, soil type, rainfall distribution, slope, geomorphological features, drainage density, elevation and lineament density parameters are considered for the delineation of anthropogenic contamination zones based on an integrated index model in Arc-GIS. Various input layers were assigned weights and then weight normalization process was adopted using Saaty’s AHP method to develop the integrated potential anthropogenic contamination zone (PACZ) map, based on the relative importance of anthropogenic contamination of groundwater. According to the proposed model majority of the study area falls under precarious zone, though certain areas fall under safe zone. In course of time, without proper planning the area could turn out to be moderately unsafe to unsafe zone. The PACZ map was validated with the fluoride concentration in groundwater as per National Rural Drinking Water Programme (NRDWP) report along with the measured nitrate concentration values. Model accuracy was achieved by agreement of about 82% of the fluoride values and 94% of the nitrate values with the proposed output map. Further validation of the model with fluoride and nitrate data was performed using computing similarity analysis with Pearson’s correlation coefficient which suggests anomalously higher concentrations of fluoride and nitrate ion concentration in certain areas of Arang block, which could be emanated from non-point anthropogenic sources. Additionally, Gibbs’s plot and saturation indices of fluorite and calcite suggest that groundwater chemistry is primarily controlled by aquifer lithological characteristics (rock–water interaction) and diffused anthropogenic contamination sources.

**Keywords** Groundwater · Potential anthropogenic contamination zone · GIS · Multi-criteria decision analysis–analytical hierarchy process · Arang block

**Electronic supplementary material** The online version of this article (<https://doi.org/10.1007/s12665-019-8724-z>) contains supplementary material, which is available to authorized users.

✉ Srinivas Pasupuleti  
srinivas@iitism.ac.in

<sup>1</sup> Department of Civil Engineering, Indian Institute of Technology (Indian School of Mines), Dhanbad, Jharkhand 826004, India

<sup>2</sup> Department of Chemical Engineering, Indian Institute of Technology (Indian School of Mines), Dhanbad, Jharkhand 826004, India

<sup>3</sup> Exploration Department, Central Mine Planning and Design Institute Limited, Bilaspur, Chhattisgarh 495006, India

<sup>4</sup> Department of Applied Geology, Indian Institute of Technology (Indian School of Mines), Dhanbad, Jharkhand 826004, India

## Introduction

Groundwater is a valuable natural resource and its worldwide availability is steadily and continuously depleting because of excessive utilization by human beings especially in certain water sensitive areas (Gleeson et al. 2012; Singh et al. 2018). Nowadays, deterioration in groundwater quality is an imminent concerns across the globe (Singh et al. 2017a, b) especially the toxic trace elements including fluoride and nitrate ion contamination of groundwater. Fluoride and nitrate ions in groundwater are found in varying concentrations, i.e., ranging from low to high which is well reported from literature. Consumption of fluoride concentration in certain proportion is vital for humans that prevent tooth decay and thereby making the tooth more acid resistant. However, when consumed in exceeding prescribed limits ( $> 1.5$  mg/L), resulting major health hazards such as dental fluorosis, skeletal fluorosis, and deformation of bones in children and adults (Amalraj and Pius 2013; Olaka et al. 2016). At a global scale, fluoride contamination in groundwater is widely encountered in China, Ethiopia, India, Iran, Jordan, Kenya, Nigeria, Pakistan, Sri Lanka, Sudan, Syria and western Brazil (Craig et al. 2015; Kumar et al. 2017). Moreover, fluoride concentration has been notified as a main concern of groundwater contaminant by the United States Environmental Protection Agency (USEPA).

Globally, various researchers also have reported incidence of nitrate concentration within groundwater in Australia, Canada, India, Iran, Morocco, Northern China, Turkey, USA, etc. (Foster and Chilton 2003; Zhou 2015; Fienen and Arshad 2016; Ward et al. 2018). The permissible limit of nitrate concentration as restricted by the Bureau of Indian Standards (BIS 2012) and USEPA 2006 is 45 mg/L. The consumption of nitrate above permissible limit ( $> 45$  mg/L) in drinking water cause methemoglobinemia for children especially below 6 months of age (Fan and Steinberg 1996; Alabdula'aly et al. 2010; Singha et al. 2017) and also various stomach and gastrointestinal health problems such as cancer and tumors (Khandare 2013; Khan and Jhariya 2017), headache, breathing trouble, multiple sclerosis and thyroid problems (Gatseva and Argirova 2008; Ahada and Suthar 2018). In India, a total of 11 states covering 95 districts are affected by consuming groundwater with nitrate concentration exceeding the prescribed limit (Kumar and Shah 2006). The occurrence of groundwater anthropogenic contamination due to fluoride and nitrate content in various parts of Chhattisgarh was also reported (GWYB 2016; Yadav et al. 2016; Khan and Jhariya 2017).

Fluoride contamination in groundwater can be from both geogenic and anthropogenic sources. Among the

geogenic sources, most common type of fluoride-bearing minerals are fluorite, apatite, biotite, and muscovite which are responsible for releasing fluoride in the groundwater system (Edmunds and Smedley 2013). Similarly, anthropogenic sources include the use of phosphate fertilizers in agricultural fields, pesticides, industrial chemical spills, burning of coal for brick kilns (Jha et al. 2011), over-extraction of groundwater, deforestation (Roy and Dass 2013; Ramteke et al. 2018) and seepage in septic tanks (Jordan and Smith 2005). Elevated nitrate concentration in groundwater is rarely contributed by the geogenic sources and mainly caused due to the contact of soil media with waste disposed water and the application of nitrate fertilizer in agricultural fields. Application of nitrogenous fertilizer, manure, animal farming and well soil drainage system are the major factors for leaching of nitrate from surface to the groundwater storage (Srivastava and Ramanathan 2018; Ducci 2018). Various litho-hydrogeological factors such as geology, soil, water table depth, geomorphology, elevation, faults or lineaments, land use–land cover, rainfall, aquifer, slope, drainage density, etc., play important role in groundwater system. Earlier workers have reported various groundwater management studies based on different hydrogeological factors with geographical information system (GIS)-based models. Using multi-criteria decision analysis–analytical hierarchy process (MCDA–AHP) technique, various studies such as delineation of groundwater potential zones (Pinto et al. 2015; Panahi et al. 2017; Akinlalu et al. 2017), identification of site selection for artificial recharge (Mehrabi et al. 2013; Al-shabeeb 2016; Kazakis 2018), groundwater vulnerability assessment (Sener and Davraz 2013; Wu et al. 2016; Xiaoyu et al. 2018) have been carried out considering different hydrogeological inputs. Till date, very few studies with limited litho-hydrogeological factors have been employed for AHP-based GIS model in the field of anthropogenic contamination zone mapping. Based on literature review, it is clear that identification of groundwater anthropogenic contamination areas has been reported either by groundwater hydro-geochemical studies or by considering hydrogeological factors alone. Therefore, the present study adds an approach for groundwater potential anthropogenic contamination (PACZ) zonation mapping using litho-hydrogeological parameters with GIS-based AHP method and identifying the actual source of anthropogenic contamination in groundwater through hydro-geochemical analysis as such studies are very limited and needs to be looked into carefully.

The present study demonstrates the GIS-based MCDA–AHP approach for a better understanding on the leading factors contributing to groundwater fluoride and nitrate contamination zones in Arang block of Raipur district, Chhattisgarh, India. The principal objectives of this

study include (1) identification and selection of the most controlling geological, hydrogeological and hydrometeorological factors that are causing groundwater anthropogenic contamination. (2) Developing a litho-hydrogeological-based model by including the selected fluoride and nitrate controlling and contributing factors thereby assigning weights and ratings based on their relative importance using GIS-based AHP approach. (3) Mapping of potential anthropogenic contamination zones of the study area. (4) Identification of actual significant source of groundwater anthropogenic contamination by hydrochemical analysis. (5) Accuracy performance of the proposed model by superimposition of fluoride and nitrate points over the final PACZ map. (6) Similarity analysis between fluoride, nitrate concentration values and respective PACZ indices. (7) Finally, comparison analysis between fluoride and nitrate concentration with land use patterns.

### Study area

Arang block is located in the eastern stretch of Raipur district, Chhattisgarh, India, and is one of the largest, fairly composed and compact shaped blocks which extends an area of 905.79 km<sup>2</sup> comprising 168 villages and 104 gram panchayats (village councils). The present study area is geographically bounded by latitudes 21°27'20" N and 21°4'37" N and longitudes 81°42'58" E and 81°11'49" E (Fig. 1), covered in the Survey of India toposheet No. 64 G. Mahanadi River is the major perennial river flowing over quartzite terrain, from South-east to North-east. Rocks mainly consist of limestone, shale, dolomite and sandstone belonging to Chhattisgarh Supergroup of Proterozoic age. Groundwater occurs in phreatic condition in the weathered mantle of these rocks, which extends up to a depth of 25 mbgl (meter below ground level). The caverns formed in limestone and dolomites holds good amount of ground water which are limited mostly to around 80 m. Limestone and dolomite form

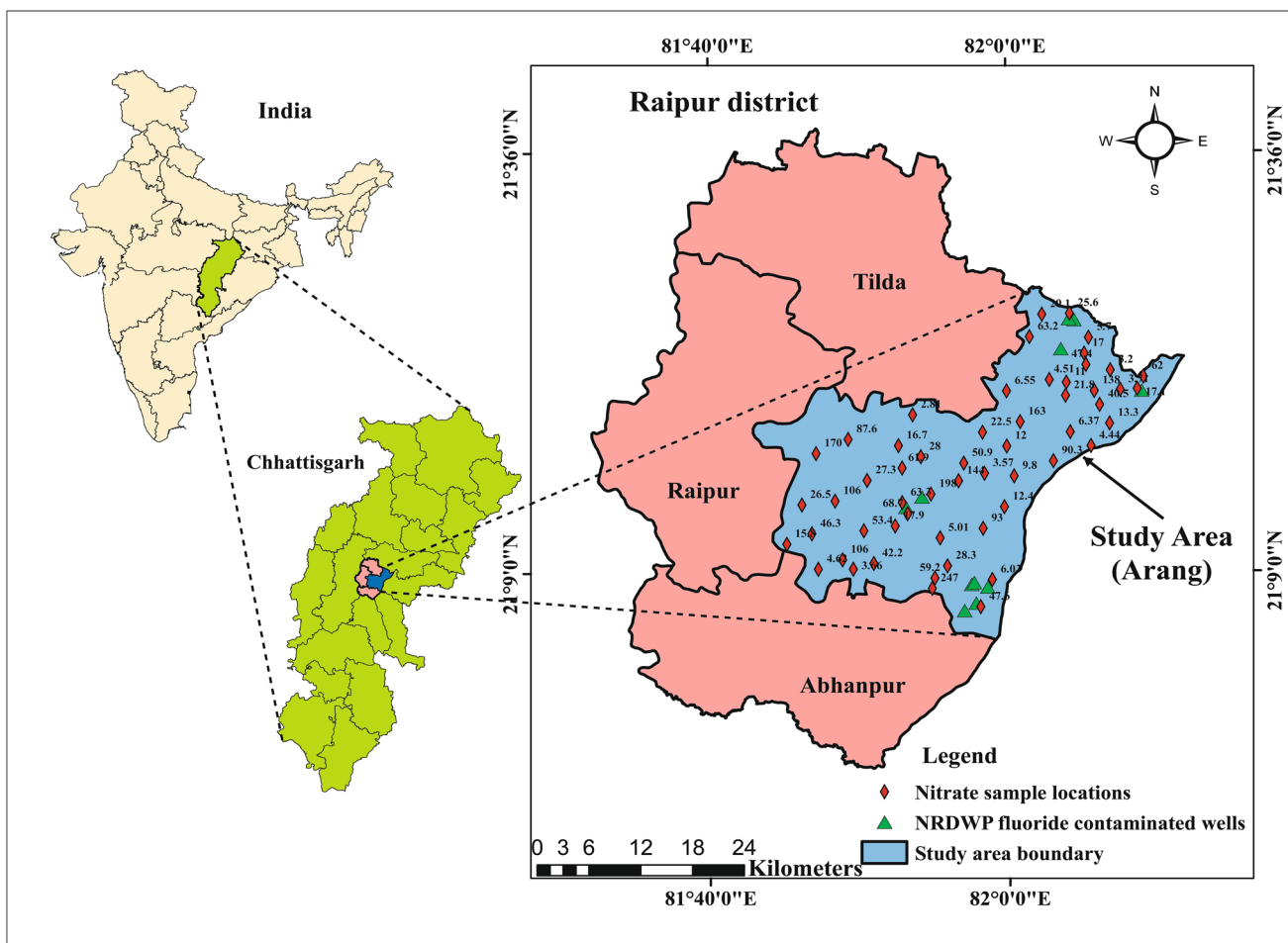


Fig. 1 Geographical location map of the study area

the main aquifer system in the area. Charmuria limestone (yield ranges 0.5–7 lps) and Gunderdehi shale (yield ranges 0.1–3 lps) are not very good yielding. Gunderdehi Formation in the study area behaves as aquiclude and thickness ranges from 60 to 120 m. Cavernous limestone of Chandi Formation forms the good aquifer (yield ranges 0.5–14 lps) in the district. The transmissivity of this formation varies 1–440 m<sup>2</sup>/day. Potential zones for Charmuria limestone, Chandi Formation and Gunderdehi Formation encountered from 25 to 85 mbgl, 17–172 mbgl and 21–66 mbgl, respectively. The alluvium blanket along the major rivers also form good repository of ground water (maximum yield 10 lps) comprise mainly gravel, coarser to medium sand and silt. The thickness of the alluvium deposits in the region varies from 10 to 20 m. The depth of water level as recorded in the year 2012 in the pre-monsoon period is 13.6 m and in post-monsoon period is 2.83 m (DSR 2016). Geologically, the study area is characterized by rocks belonging to Proterozoic age, limestone and dolomite being the dominant rocks followed by laterite and soils ranging age between sub-recent to recent formations. Ultisols and vertisols are the two major soil groups found in Arang block. Paddy is the major kharif crop cultivated with largest sown area (658.06 km<sup>2</sup>) followed by pulses and wheat in the entire study area (DSR 2016). Groundwater is the prime source for domestic purposes and nearly 75% of the rural population is totally dependent on groundwater. The stage of groundwater development estimated in the year 2009 for the study area is 35.51% (CGWB 2013). Climatically, the district experiences a tropical wet and dry climate and the temperature varies in between a maximum of 45 °C (May and June) to a minimum of 13 °C (December and January) annually. The normal annual rainfall in the district is 1319 mm and the average is 1323 mm as recorded in the year 2011 responsible mainly due to the South-west monsoon. Based on the collected data of last 35 years, the average annual rainfall is 1260 mm in the study area.

## Materials and methods

### Data source and preparation of thematic maps

Geomorphology, soil and lithological (geology and aquifer media) data were obtained from Chhattisgarh Infotech Promotion Society (CHIPS), Raipur. Hydrological data such as groundwater table (2017, pre-monsoon period) and rainfall (35 years) were collected from CGWB official website (<http://cgwb.gov.in/GW-data-access.html>) and State Data Centre, Raipur, respectively. Lineament map was prepared using collected satellite images, digital elevation model (DEM) and aerial photographs from the official portal of Bhuvan (<http://bhuvan.nrsc.gov.in/>) and National Remote

Sensing Centre (NRSC). Slope map, elevation map and drainage density map were prepared from collected DEM with a resolution of 30 m from Bhuvan official portal. Land use–land cover map was prepared from the published map of the district survey report of the year 2016. Various water quality parameters (pH, EC, TA, TH, Ca<sup>2+</sup>, Mg<sup>2+</sup>, Na<sup>+</sup>, Fe<sup>2+</sup>, K<sup>+</sup>, HCO<sub>3</sub><sup>-</sup>, Cl<sup>-</sup>, SO<sub>4</sub><sup>2-</sup>, F<sup>-</sup>, and SiO<sub>2</sub>) were obtained from CGWB year book 2016–2017, to study the groundwater hydro-geochemistry of the Arang block. A total of 11 groundwater with some fluoride concentration (obtained from contamination report of National Rural Drinking Water Programme, NRDWP, 2016–2017) and 55 locations of measured groundwater nitrate values were considered for model validation purpose. Groundwater nitrate concentrations of 55 locations were measured during May 2019 by nitrate ion electrode method using ion meter (model 781 of Metrohm made). All the thematic layers were initially prepared in the form of shape file (.shp) and later on converted to raster format in Arc-GIS 10.3. The methodology undertaken for the study area is shown in Fig. 2.

### Allocating weights and ranks to the thematic layers and respective subclasses

#### Relative information of various controlling factors

Usually superficial aquifers are permeable and unconfined in nature; thus are highly vulnerable to anthropogenic contamination (Javadi et al. 2011a, b). The leaching of anthropogenic contamination depends on the permeability of aquifer material. Quaternary alluvium (unconsolidated) is the composition of gravel, sand, silt and clay with high infiltration capacity which promotes leaching of anthropogenic contamination to the aquifer. The shallow lateritic formation is highly permeable in rainy season that makes shallow groundwater highly susceptible to surface contamination (Bonsor et al. 2014). Similarly cavernous limestone of Chandi Formation and Charmuria Limestone (semi-consolidated) bears high permeability and porosity, forms the potential aquifer in the study area as compared to the Gunderdehi shale Formation (CGWB 2011). Hence, limestone aquifers are also susceptible to surface source contamination in the region. Phosphatic fertilizers causes the major source of anthropogenic fluoride contamination in groundwater through leaching (Dartan and Taspinar 2017; Ramteke et al. 2018). Soil alkalization mainly occurs due to intensive agricultural practice with phosphatic fertilizer and organic manure which results in the availability of high fluoride concentration in the groundwater (Ayoob and Gupta 2006). Significant positive correlation between application of phosphatic fertilizer and fluoride concentration and its subsequent leaching may also lead to high concentration of fluoride in groundwater (Kundu and Mandal 2009). The

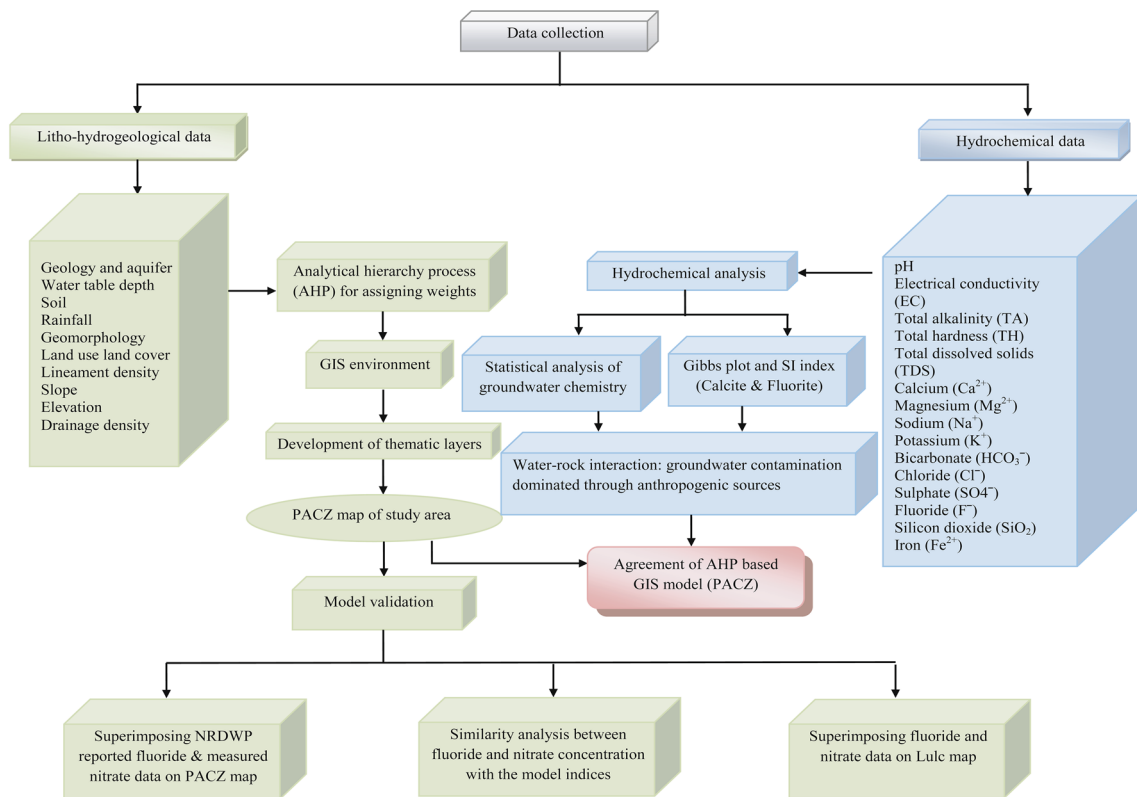
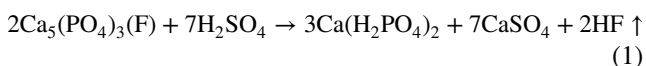


Fig. 2 Flowchart of the methodology followed for the study area

water hardness level, pH and soil with the clayey material mainly govern the transportation as well as the transformation of fluoride in the soil. By displacing hydroxide from the clay surface, fluoride binds to clay particles (Meeussen et al. 1996). Single superphosphate (SSP) which is well-known phosphatic fertilizer and the manufacture of this fertilizer involves the following equation:



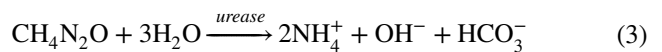
After the reaction of mobilized fluoride with calcium it forms CaF<sub>2</sub>:



The further dissolution of fluorite (CaF<sub>2</sub>) in groundwater environment enhances the fluoride concentration. Normally, soluble fluoride content present in the phosphatic fertilizer is 60–250 mg/kg with the average content of 175 mg/kg (Farooqi et al. 2007).

Groundwater anthropogenic contamination depends on the soil texture, irrigation and amount of rainfall. Sandy soil is responsible for nitrate leaching as compared to the clay (Boumans et al. 2008) with higher the annual rainfall, higher is the nitrate leaching (Goolsby et al.

1997; Huang et al. 2017). The intensity of leaching is generally more in sandy type of soil under high irrigation or high rainfall (Elfaki 2010). Extensive application of nitrogenous fertilizer especially urea (CH<sub>4</sub>N<sub>2</sub>O) for the high-yielding crops in agricultural field plays a vital role for elevated concentration of nitrate in groundwater. The occurrence of leached nitrate through urease which is very much common in clay particles, soil microbes and plant residues and is summarized in Eqs. 3 and 4:



The ammonium (NH<sub>4</sub><sup>+</sup>) further oxidized with the available oxygen in soil to form the NO<sub>2</sub> and finally NO<sub>3</sub>:



Moreover, leaching of nitrate from the unsaturated deposits is very common as nitrate is negatively charged high soluble ion and results in higher mobility of nitrate into the aquifer (Vinod et al. 2015). Flat ground surface promotes to high infiltration because of its less drainage density which may lead to higher leaching of fluoride and nitrate in the subsurface water system.

### Assigning weights and ranks to the parameters

The litho-hydrogeological-based GIS model was developed by considering the parameters namely, geological and aquifer characteristics, land use–land cover, depth to water table, soil type, distribution of rainfall, geomorphology, drainage density, slope, elevation and lineament density. Each parameter was assigned weightage between

1 and 10 and the subclasses of each parameter were further assigned with rating according to their importance on nitrate and fluoride contamination. Ratings and weights were assigned based on the previously published documents, knowledge base information and conditions favorable for anthropogenic groundwater contamination. The most significant parameter leading to higher anthropogenic

**Table 1** Normalized weight, ratings and areal extent of litho-hydrogeological parameters using AHP process

Parameter	Classification	Weight	Normalized weight	Rating	Area	% Area weight
Geology and aquifer (G)	Cavernous limestone of Chandi Formation	10	0.27	6	167.47	18.49
	Gunderdehi shale Formation			4	311.33	34.37
	Charmuria limestone Formation			7	337.67	37.28
	Laterite (cenozoic)			9	53.39	5.90
	Alluvium-(quaternary)			10	35.93	3.96
Land use–land cover (Lulc)	Agricultural land	9	0.18	9	751.27	82.94
	Built-up area (rural)			5	60.76	6.70
	Built-up area (urban)			7	2.43	0.27
	Waste land			1	36.66	4.05
	Water body			2	54.67	6.04
Depth to water table (DWT) (m)	<4	8	0.12	8	361.69	39.93
	4–8			6	538.30	59.43
	>8			4	5.80	0.64
Soil (S)	Clayey loam	8	0.12	5	596.89	65.89
	Clay			4	155.97	17.22
	Sandy clay loam			6	104.88	11.58
	Gravelly sand clay loam			7	33.94	3.75
	Sandy loam			8	14.11	1.56
Rainfall (R) (mm/year)	<1200	7	0.10	5	235.52	26.00
	1200–1300			6	384.98	42.50
	>1300			7	285.29	31.50
Geomorphology (GM)	Pediment	6	0.06	6	391.57	43.22
	Buried pediment			3	236.66	26.13
	Flood plain			4	205.04	22.65
	Valley fill			4	18.17	2.00
	Alluvium plain complex			5	54.35	6.00
Drainage density (DD) (km/sq.km)	0–0.45	4	0.05	4	187.30	20.68
	0.45–0.90			3	326.47	36.04
	0.90–1.30			2	250.30	27.63
	1.30–2.32			1	141.72	15.65
Slope (T) (degree)	0–4	4	0.06	4	855.64	94.46
	4–10			2	48.61	5.37
	>10			1	1.54	0.17
Elevation (E) (m)	225–285	3	0.02	3	612.11	67.58
	285–300			2	207.18	22.87
	>300			1	86.50	9.55
Lineament density (LD) (km/sq.km)	0.50–1.13	3	0.02	3	74.16	8.19
	0.18–0.50			2	272.67	30.10
	0–0.18			1	558.96	61.71

pollution in groundwater was assigned higher ratings (10) and the least was assigned a rating of 1 (Table 1).

**Normalization of weights using AHP method**

MCDA techniques have been proved to be most efficient tools in providing solutions to the various water resource problems associated for its sustainable management for more than 20 years (Hatefi Ardakani and Ekhtesasi 2016; Jenifer and Jha 2017). AHP is one of the widely adopted methods of MCDA technique that helps in decision-making while selecting options for assigning appropriate weights and rates in a spatial domain in the model. AHP for the first time was introduced by Saaty (1980) for helping different resource managers dealing with various socio-economic decision-making problems.

Thematic maps have been developed for all the ten parameters selected for the study and their relationships among each other has been derived using AHP method. AHP technique proves successful in the case, when parameters are independent and gives the impacts of distribution among the parameters/factors with ratio scale priority

vectors for better judgment (Alonso and Lamata 2006; Jhariya et al. 2016). The application of AHP process basically involves three dominant steps: (1) disintegration, or construction of hierarchy; (2) data execution and collection to provide pair-wise comparison in hierarchy arrangement; and (3) combination of priorities (Harker and Vargas 1987). This method computes the normalized weights for each parameter by preparing a square matrix where all the parameters are compared with each other on the basis of their importance on the other parameter. To obtain this square matrix, a pair-wise comparison matrix was formed and the relative importance values were examined based on Satty’s 1–9 point scale (Table 2), where minimum point scale (1) and maximum point scale (9) reflects equal importance and extreme importance, respectively, between two thematic layers (Saaty 1980). The diagonal elements of the matrix show 1. The pair-wise comparison matrix (Table 3) constructed for the input layers is as follows:

$$X = \begin{pmatrix} r_{11} & r_{12} & \dots & r_{1j} \\ r_{21} & r_{22} & \dots & r_{2j} \\ \vdots & \vdots & \ddots & \vdots \\ r_{i1} & \dots & \dots & r_{ij} \end{pmatrix} \tag{5}$$

The computed pair-wise comparison matrix ( $X = [r_{ij}]$ ) is normalized by the following equation:

$$r_{ij}^* = \frac{r_{ij}}{\sum_{i=1}^n r_{ij}} \tag{6}$$

for all  $j = 1, 2, 3, 4, \dots, n$ ,  $r_{ij}$  is the element of  $i$  row and  $j$  column of matrix.

The normalized weight ( $w_i$ ) is calculated utilizing Eq. 7 and shown in Table 4:

$$w_i = \frac{\sum_{j=1}^n r_{ij}^*}{n} \tag{7}$$

**Table 2** Saaty’s 1–9 point intensity of relative importance scale

Scale	Importance
1	Equal importance
3	Moderate importance of one over another
5	Strong importance
7	Very strong importance
9	Extreme importance
2, 4, 6, 8	Intermediate values between the two adjacent judgments
Reciprocals of the above nonzero numbers	Reciprocal for inverse comparison

Source: Saaty (1980)

**Table 3** Pair-wise comparison matrix of key ten factors for AHP process

Parameters	P1	P2	P3	P4	P5	P6	P7	P8	P9	P10
P1	1.00	2.00	3.00	3.00	4.00	5.00	5.00	5.00	6.00	6.00
P2	0.50	1.00	2.00	2.00	3.00	4.00	4.00	4.00	5.00	5.00
P3	0.33	0.50	1.00	1.00	2.00	2.00	3.00	3.00	4.00	4.00
P4	0.33	0.50	1.00	1.00	2.00	3.00	3.00	2.00	4.00	4.00
P5	0.25	0.33	0.50	0.50	1.00	3.00	3.00	3.00	4.00	4.00
P6	0.20	0.25	0.50	0.33	0.33	1.00	2.00	2.00	3.00	3.00
P7	0.20	0.25	0.33	0.33	0.33	0.50	1.00	1.00	4.00	4.00
P8	0.20	0.25	0.33	0.50	0.33	0.50	1.00	1.00	4.00	4.00
P9	0.17	0.20	0.25	0.25	0.25	0.33	0.25	0.25	1.00	1.00
P10	0.17	0.20	0.25	0.25	0.25	0.33	0.25	0.25	1.00	1.00

P1 geology and aquifer, P2 Lulc, P3 depth to water table, P4 soil, P5 rainfall, P6 geomorphology, P7 drainage density, P8 slope, P9 elevation, P10 lineament density

**Table 4** Scores/weights of ten key parameters for AHP process

Parameters	P1	P2	P3	P4	P5	P6	P7	P8	P9	P10	Weights
P1	0.30	0.36	0.33	0.33	0.30	0.25	0.22	0.23	0.17	0.17	0.27
P2	0.15	0.18	0.22	0.22	0.22	0.20	0.18	0.19	0.14	0.14	0.18
P3	0.10	0.09	0.11	0.11	0.15	0.10	0.13	0.14	0.11	0.11	0.12
P4	0.10	0.09	0.11	0.11	0.15	0.15	0.13	0.09	0.11	0.11	0.12
P5	0.07	0.06	0.05	0.05	0.07	0.15	0.13	0.14	0.11	0.11	0.10
P6	0.06	0.05	0.05	0.04	0.02	0.05	0.09	0.09	0.08	0.08	0.06
P7	0.06	0.05	0.04	0.04	0.02	0.03	0.04	0.05	0.11	0.11	0.05
P8	0.06	0.05	0.04	0.05	0.02	0.03	0.04	0.05	0.11	0.11	0.06
P9	0.05	0.04	0.03	0.03	0.02	0.02	0.01	0.01	0.03	0.03	0.03
P10	0.05	0.04	0.03	0.03	0.02	0.02	0.01	0.01	0.03	0.03	0.03

P1 geology and aquifer, P2 Lulc, P3 depth to water table, P4 soil, P5 rainfall, P6 geomorphology, P7 drainage density, P8 slope, P9 elevation, P10 lineament density

for all  $i = 1, 2, 3, 4, \dots, n$ .

The AHP method helps to decide and reduce the uncertainty in judgments with the aid of principal eigen-value and the consistency index as proposed by Saaty (2004). Saaty’s proposed index for computation of consistency is known as consistency index (CI) which is computed using Eq. 8:

$$CI = \frac{\lambda_{max} - n}{n - 1}, \tag{8}$$

where  $n$  = total number of parameters (10) and  $\lambda_{max}$  = mean consistency eigenvector value.

Consistency ratio (CR) is determined which signifies the degree of consistency of pair-wise comparison matrix is obtained by Eq. 9:

$$CR = \frac{CI}{RI} \tag{9}$$

where CI is the consistency index and RI is the random/ratio index. The respective RI values for different “ $n$ ” parameters as proposed by Saaty (2007) are shown in Table 5. The CR value obtained was 5.5% which is less than 10%, thus justifying the consistency of the weights chosen (Saaty 1980).

**Weighted overlay index technique (WOIT)**

The widely adopted index overlay method was utilized by various researchers in the area of groundwater investigation from different locations (Senanayake et al. 2016; Al-Abadi et al. 2017; Singha et al. 2017). The rates and weights were multiplied for each factor and added together to produce potential

anthropogenic contamination zone (PACZ). Hence, the PACZ for the study area was computed by the summation of the products of rating and weights of each factor by using Eq. 10:

$$PACZ = \sum_1^n (X_r Y_w), \tag{10}$$

where  $X$  and  $Y$  indicate the parameters and subscript  $r$  and  $w$  are the respective ratings assigned to parameter subclasses and weights to each parameter class.

**Groundwater chemistry and governing process of the study area**

**Gibbs diagram**

Gibbs plot (Gibbs 1970) is widely popular to distinguish the impact of three distinct fields of dominance which are mainly precipitation, rock–water and evaporation on groundwater chemistry. A total of 14 numbers of point location data from Central Groundwater Board’s yearbook (2016–2017) for Arang block, within the study area, were selected to construct the Gibbs’s plot. The ratio of  $Na^+$  to  $(Na^+ + Ca^{2+})$  and  $Cl^-$  to  $(Cl^- + HCO_3^-)$  and TDS as the components were used to construct the Gibbs diagram. The TDS concentrations computed from the groundwater EC values using Eq. 11 as suggested by Rusydi (2018):

$$TDS = 0.7 * EC. \tag{11}$$

**Table 5** Saaty’s ratio index (RI) for various number of parameters ( $n$ )

$n$	1	2	3	4	5	6	7	8	9	10	11	12
RI	0	0	0.58	0.89	1.12	1.25	1.32	1.41	1.45	1.49	1.52	1.54

Source: Saaty (2007)



## Saturation index (SI)

Saturation index with respect to a mineral indicates the thermodynamic stability of groundwater (Chidambaram et al. 2011). Groundwater chemical data (CGYB, 2016–17) of 14 locations from various parts of Arang block were considered to compute the SI value of fluorite ( $\text{CaF}_2$ ) and calcite ( $\text{CaCO}_3$ ) using PHREEQC version 2 (Parkhurst and Appelo 1999). The calculation of SI is based on the following equation (Appelo and Postma 2005):

$$SI = \log \left( \frac{IAP}{K_{sp}} \right), \quad (12)$$

where SI refers to the saturation index of minerals, IAP represents the ion activity product of the dissociated chemical species in solution and  $K_{sp}$  is the equilibrium solubility product. Finally, SI values of both the minerals were plotted for better visual interpretation of the groundwater chemistry the area.

## Results and discussion

### Lithological and hydrogeological factors

The occurrence of groundwater and its quality deterioration are related to geological and aquifer characteristics, land use–land cover, depth to water table, soil type, rainfall, geomorphology, drainage density, slope, elevation and lineament features of the region. The discharge of minerals from geological units into groundwater through rock–water interaction plays significant role resulting in changes in groundwater quality. The study area was categorized into five geological (G) subclasses: i.e., cavernous limestone of Chandi Formation, Charmuria limestone Formation, Gunderdehi shale Formation, Laterite (Cenozoic), and Quaternary (alluvium) extending over an area of about 167.44 km<sup>2</sup>, 311.08 km<sup>2</sup>, 338.27 km<sup>2</sup>, 35.51 km<sup>2</sup>, and 53.49 km<sup>2</sup>, respectively. Geology and aquifer map of Arang block is shown in Fig. 3a.

Groundwater infiltration rate in an area is also greatly influenced by land use–land cover (Lulc) patterns of the region which in turn may increase groundwater recharge or vice versa (Chaudhary and Kumar 2018). The whole study area was categorized into five land use–land cover patterns, namely agricultural land, built-up area (rural), built-up area (urban), wasteland and water body covering an area of 751.27 km<sup>2</sup>, 60.76 km<sup>2</sup>, 2.43 km<sup>2</sup>, 36.66 km<sup>2</sup> and 54.67 km<sup>2</sup>, respectively. Majority of the study area is surrounded by agricultural land (82.94%) which also may be attributed as one of the anthropogenic sources for discharging fluoride and nitrate through leaching from chemical fertilizers into

the groundwater. The land use–land cover map of Arang block is shown in Fig. 3b.

The depth to water table (DWT) of a region depends on hydrogeological conditions of the area, topography, rainfall, soil type, etc. (Elewa and Qaddah, 2011). As shown in Fig. 3c, the groundwater table depth in the study area was classified into three subclasses viz., less than 4 m (361.69 km<sup>2</sup>) in central southern and a small patch in western portion, 4–8 m (538.30 km<sup>2</sup>) in majority portion of the study area and finally a small patch with more than 8 m (5.80 km<sup>2</sup>) in western part of Arang block is demarcated.

Soil type (S) of an area indicates the holding capacity of water and their permeability (Avtar et al. 2010) through which the contaminants can take longer time to travel and reach the groundwater. In the study area, clay soil and clayey loam occupies the major portion (155.97 km<sup>2</sup> and 596.89 km<sup>2</sup>), whereas gravelly sand clay loam covers an area of 33.9 km<sup>2</sup>, sandy clay loams covers an area of 104.88 km<sup>2</sup> and sandy loam extends over an area of 14.11 km<sup>2</sup>. The soil map of Arang block is shown in Fig. 3d.

Rainfall distribution (R), intensity and its duration in an area play a major role in infiltration. Higher the rainfall intensity shorter is the duration which indicates that higher surface runoff with less infiltration, whereas low intensity with longer duration reduces surface runoff and increases groundwater infiltration and (Ibrahim-Bathis and Ahmed 2016) thereby contributing to rise of contamination rate in subsurface water. The distribution of rainfall in the study area was categorized into three subclasses: i.e., less than 1200 mm is experienced in an area of 235.52 km<sup>2</sup>, an area of 384.98 km<sup>2</sup> is experienced with 1200–1300 mm rainfall and more than 1300 mm rainfall is observed in 285.29 km<sup>2</sup>, respectively. The annual rainfall ranges from 1173 to 1364 mm. The rainfall distribution map of Arang block is shown in Fig. 3e.

The geomorphic patterns (GM) of an area indicate information related to groundwater conditions, its occurrence, different landforms (Nag and Kundu 2018), underlying geological units, structural fractures, etc., and therefore is selected as one of the significant parameters of groundwater studies (Thapa et al. 2017). Geomorphologically, the study area is categorized into five subclasses, namely, pediment encompasses an area of 391.57 km<sup>2</sup>, buried pediment with an area of 236.66 km<sup>2</sup>, flood plain covers an area of 205.04 km<sup>2</sup>, valley fill covers an area of 18.17 km<sup>2</sup> and alluvium plain complex covers an area of 54.35 km<sup>2</sup>. The geomorphology map of Arang block is shown in Fig. 3f.

Drainage density (DD) and permeability are conflicting in function to each other, higher drainage density indicates low permeability (Nag and Kundu 2018) thereby indicating a lower rate of contaminants to infiltrate and contrariwise. Drainage density was classified into four subclasses, i.e., very low (0–0.45 km/km<sup>2</sup>) accounts with 187.30 km<sup>2</sup> area,

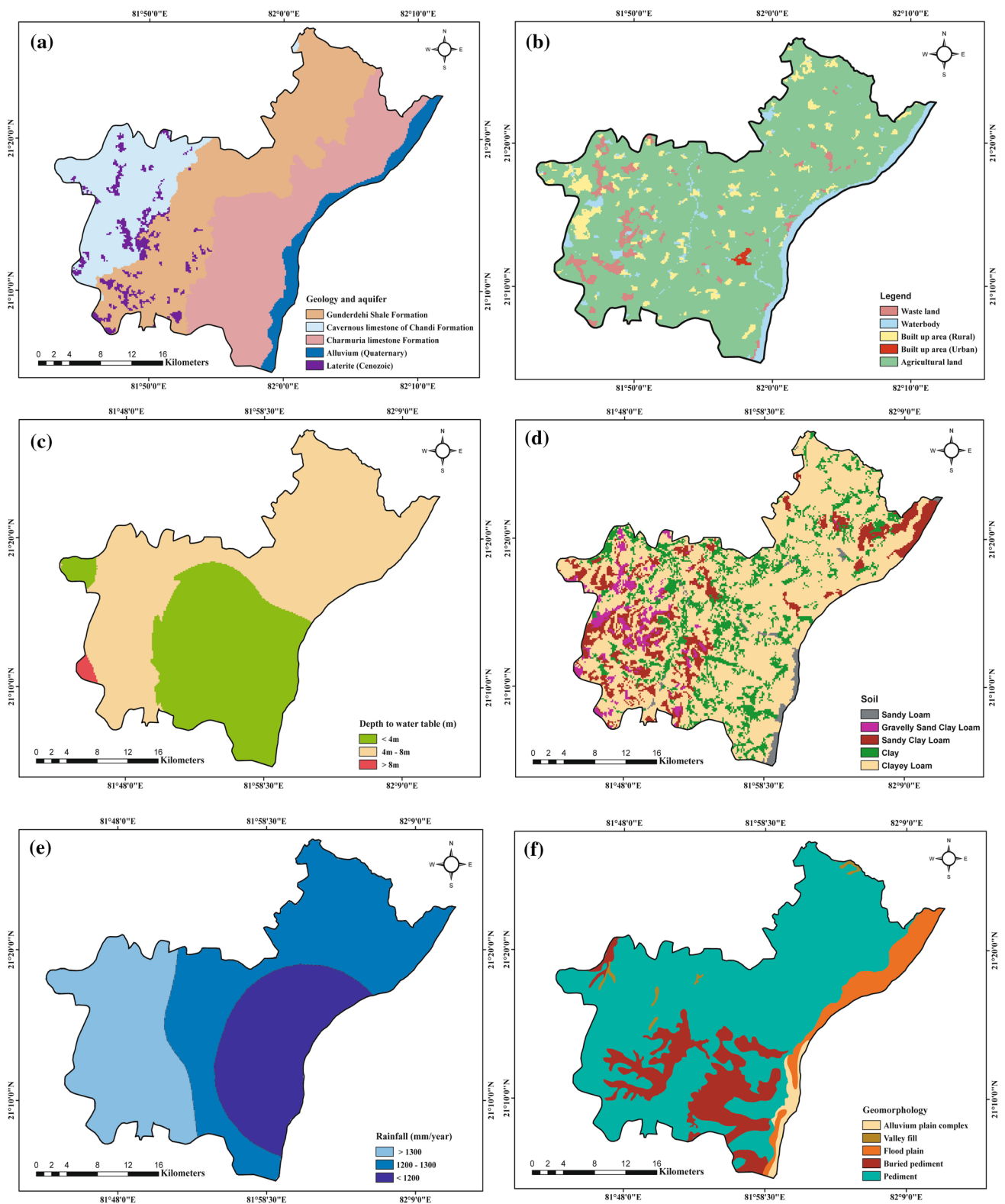


**Fig. 3** Spatial distribution map of **a** geology and aquifer. **b** Land use–land cover. **c** Depth to water table. **d** Soil type. **e** Rainfall distribution. **f** Geomorphology. **g** Drainage density. **h** Slope. **i** Elevation. **j** Lineament density of the study area

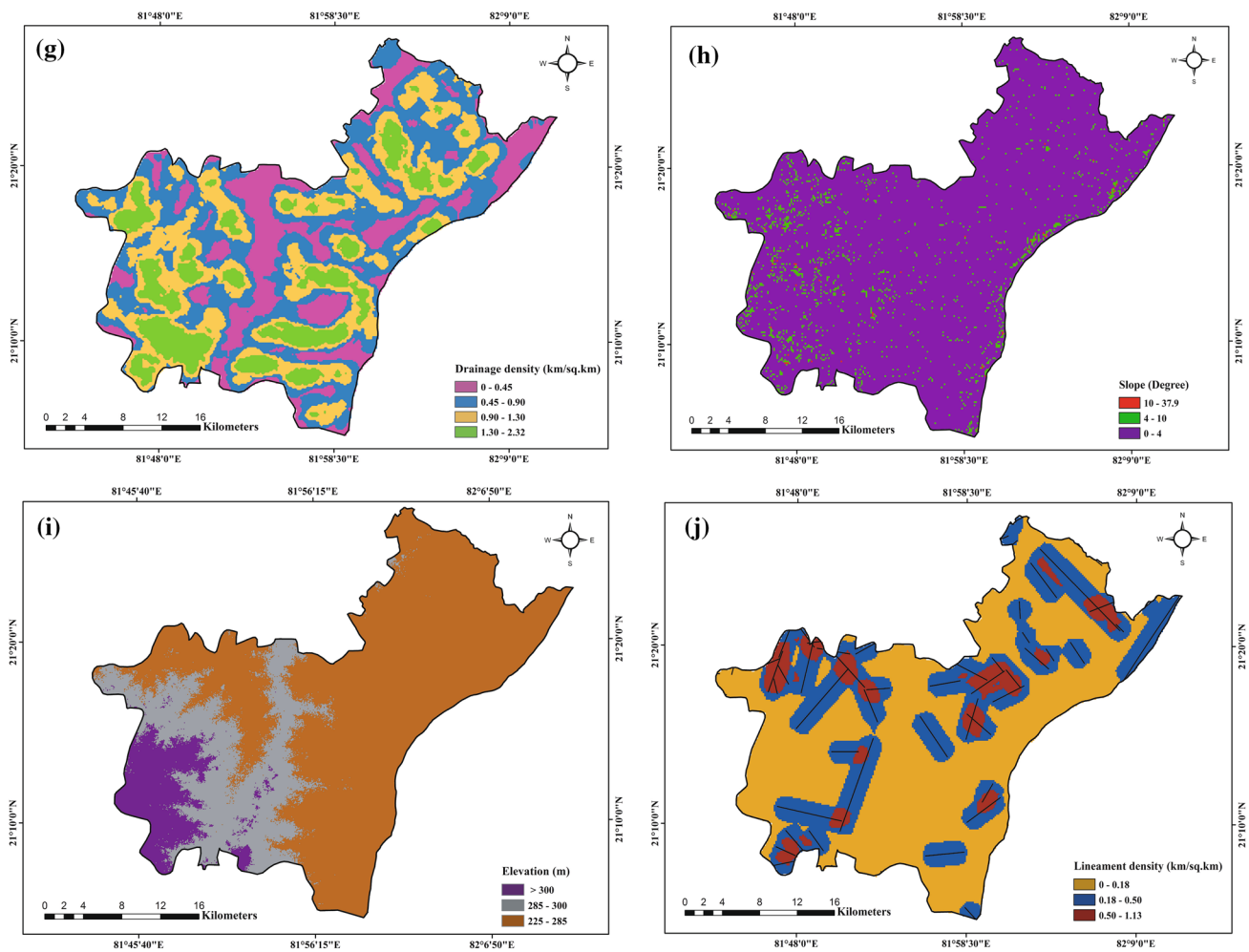


Fig. 3 (continued)

low (0.45–0.90 km/km<sup>2</sup>) with 326.47 km<sup>2</sup>, 250.30 km<sup>2</sup> with moderate (0.90–1.30 km/km<sup>2</sup>) and high drainage density (1.30–2.32 km/km<sup>2</sup>) covers an area of 141.72 km<sup>2</sup>, respectively, in the study area. The drainage density map of Arang block is shown in Fig. 3g.

The slope (T) of a region is one of the leading factors which influences groundwater recharge, i.e., a gentle slope will have low surface runoff thereby greater the rate of infiltration along with an increase in groundwater contamination and vice versa (Das et al. 2017). In the study area, the slope was grouped into three subclasses, i.e., low, moderate and high. A major portion of the study area with 855.64 km<sup>2</sup> falls within low slope area (0°–4°), moderate slope (4°–10°) covers 48.61 km<sup>2</sup> and areas with higher slope (10°–37.9°) accounts for hardly 1.53 km<sup>2</sup>. The slope map of Arang block is shown in Fig. 3h.

Areas with lower elevation tend to increase groundwater recharge as the duration of water to retain on surface

increases and vice versa (Thapa et al. 2017). Elevation (E) in the study area was categorized into three subclasses, i.e., 612.11 km<sup>2</sup> falls within 225–285 m elevation, 207.18 km<sup>2</sup> falls within 285–300 m elevation and 86.50 km<sup>2</sup> falls under higher than 300 m elevation. The elevation map of Arang block is shown in Fig. 3i.

Lineament density (LD) in an area indirectly signifies a permeable zone, i.e., the presence of fractures/lineaments become a path for movement of groundwater (Murasingh and Jha 2013), moreover may increase the rate of groundwater contamination. Lineament density in the study area was grouped in three subclasses, i.e., High fault density (0.50–1.13 km/km<sup>2</sup>) encompasses an area of 74.16 km<sup>2</sup>, moderate density (0.18–0.50) km/km<sup>2</sup> covers an area of 272.67 km<sup>2</sup>, low fault density (0–0.18 km/km<sup>2</sup>) extends an area of 558.96 km<sup>2</sup>. The lineament density map of Arang block is shown in Fig. 3j.

## Major ion chemistry and dominant hydro-geochemical process

### Groundwater quality statistics of the study area

The groundwater chemistry data of study area were obtained from Central Ground Water Year Book (CGYB) 2016–2017, CG, are shown in Table 6. It presents the overall general statistical characteristics of groundwater chemistry of the study area where the mean concentration of major ions in the study area follow the order of  $\text{Na}^+ > \text{Ca}^{2+} > \text{Mg}^{2+} > \text{K}^+$  and  $\text{HCO}_3^- > \text{Cl}^- > \text{SO}_4^{2-} > \text{F}^-$ , respectively, for cations and anions. High standard deviation of cations such as  $\text{Ca}^{2+}$  and  $\text{Na}^+$  and anions such as  $\text{HCO}_3^-$ ,  $\text{Cl}^-$  and  $\text{SO}_4^{2-}$  in groundwater, within the study area, indicates the higher degree of variability. The pH value indicates that groundwater in the Arang block is alkaline, ranges from 7.32 to 8.02. The minimum and maximum values of electrical conductivity (EC) and total alkalinity (TA) vary from 276 to 1120  $\mu\text{S}/\text{cm}$  and 80–365 mg/L, respectively. The overall total hardness (TH) in the study area varies from 20 to 295 mg/L. The  $\text{Ca}^{2+}$ ,  $\text{Mg}^{2+}$ ,  $\text{Na}^+$  and  $\text{K}^+$  concentrations range from 4 to 78 mg/L, 1.2–30 mg/L, 6.7–253.5 mg/L and 0.3–31 mg/L, respectively. In the study area,  $\text{HCO}_3^-$  and  $\text{Cl}^-$  content varies from 98 to 445 mg/L and 14.2–156.2 mg/L, respectively. The  $\text{SO}_4^{2-}$  concentration is found in Arang block, ranges from 0.1 to 143.7 mg/L and  $\text{F}^-$  vary from 0.5 to 1.9 mg/L. The  $\text{SiO}_2$  and  $\text{Fe}^{2+}$  concentrations in groundwater of Arang block ranges from 5.7 to 25 mg/L and 0.023–18.3 mg/L, respectively.

Pearson correlation coefficient matrix was performed among the various constituents of groundwater of Arang block (Table 7). The correlation of  $\text{F}^-$  with  $\text{Ca}^{2+}$  and  $\text{Mg}^{2+}$  found from this matrix reflects a negative relationship, whereas there exists a significant positive correlation ( $> 0.6$ ) of  $\text{F}^-$  with TA,  $\text{HCO}_3^-$ , and  $\text{Na}^+$ . Many researchers have also reported that  $\text{F}^-$  is inversely related to  $\text{Ca}^{2+}$  (Raj and Shaji 2017; Kumar et al. 2018) and strongly related to alkalinity (Reddy et al. 2010; Jabal et al. 2014). The relationship between  $\text{F}^-$  and  $\text{Ca}^{2+}$  is influenced by the overall groundwater quality such as pH level and the ionic strength, which results in the different types of geochemical processes that can occur (Rafique et al. 2015). In order to trace the governing hydrochemical process dominating the groundwater chemistry of the study area analytical data of 14 locations in meq/L were imported into the Gibbs plot. The output of Gibbs plot (Fig. 4a, b) clearly indicates that, majority of points fall within the field rock-water dominance. This implies that the interaction of percolating water with the host rock/aquifer present in the area governs the composition of subsurface water and which in turn triggers to elevated concentrations of TA,  $\text{HCO}_3^-$  and  $\text{Na}^+$  in groundwater of the study area, besides ion exchange process. Furthermore, Fig. 5 represents the SI values of fluorite and calcite in the

**Table 6** Statistics of groundwater chemistry ( $n = 14$  no. locations) of study area

Parameters	Minimum	Maximum	Mean	Median	Standard deviation
pH	7.32	8.02	7.62	7.63	0.18
EC ( $\mu\text{S}/\text{cm}$ )	276.0	1120.0	645.0	691.0	211.3
TA (mg/L)	80.0	365.0	174.0	157.5	82.9
TH (mg/L)	20.0	295.0	167.0	167.5	84.0
$\text{Ca}^{2+}$ (mg/L)	4.0	78.0	42.7	45.0	24.5
$\text{Mg}^{2+}$ (mg/L)	1.2	30.0	14.4	12.0	9.8
$\text{Na}^+$ (mg/L)	6.7	253.5	64.2	41.1	66.5
$\text{Fe}^{2+}$ (mg/L)	0.0	18.3	4.0	0.3	7.0
$\text{K}^+$ (mg/L)	0.3	31.0	4.8	1.7	8.2
$\text{HCO}_3^-$ (mg/L)	98.0	445.0	212.4	192.0	101.1
$\text{Cl}^-$ (mg/L)	14.2	156.2	72.8	58.6	47.3
$\text{SO}_4^{2-}$ (mg/L)	0.1	143.7	36.4	24.9	38.1
$\text{F}^-$ (mg/L)	0.5	1.9	0.9	0.8	0.5
$\text{SiO}_2$ (mg/L)	5.7	25.0	15.1	14.5	5.9

study area. The plot shows that baring a sample, most of the samples fall in the calcite equilibrium zone and fluorite under-saturation zone. Presence of dolomite and calcite minerals mainly controls the groundwater geochemistry of the study area. Groundwater in the study area is mostly in an equilibrium condition with respect to calcite, however, the dominance of  $\text{Na}^+$  over  $\text{Ca}^{2+}$  reported could be due to precipitation of calcite mineral at high pH conditions and cation exchange process (i.e., replacement of  $\text{Ca}^{2+}$  by  $\text{Na}^+$ ) in the groundwater. The SI value of fluorite clearly indicates the absence of fluoride-bearing minerals in the host rock of the study area (CGWB 2014) and also deduces adding fluoride into the groundwater system through anthropogenic activity.

### Potential anthropogenic contamination zonation map (PACZ)

The potential anthropogenic contamination zone map is developed using Arc-GIS 10.3 software by integrating all the respective thematic layers through a weighted overlay index technique according to Eq. 13:

$$PACZ = \sum_1^n G_r G_w + Lulc_r Lulc_w + DWT_r DWT_w + S_r S_w + R_r R_w + GM_r GM_w + DD_r DD_w + T_r T_w + E_r E_w + LD_r LD_w \quad (13)$$

Here the uppercase letters represent each parameter/thematic layers and subscripts 'r' and 'w' represents ratings and weights assigned to respective layers.

The index values of PACZ map (Fig. 6a) varies from 3.96 to 7.62 and the developed map was further classified into three subclasses using natural breaks process (Jenks), namely safe (3.96–5.62), moderate (5.62–6.14) and risk zone

**Table 7** Pearson correlation matrix of groundwater chemistry of the study area

Variables	pH	EC ( $\mu\text{S}/\text{cm}$ )	TA (mg/L)	TH (mg/L)	Ca <sup>2+</sup> (mg/L)	Mg <sup>2+</sup> (mg/L)	Na <sup>+</sup> (mg/L)	Fe <sup>2+</sup> (mg/L)	K <sup>+</sup> (mg/L)	HCO <sub>3</sub> <sup>-</sup> (mg/L)	Cl <sup>-</sup> (mg/L)	SO <sub>4</sub> <sup>2-</sup> (mg/L)	F <sup>-</sup> (mg/L)	SiO <sub>2</sub> (mg/L)	
pH	1.00														
EC ( $\mu\text{S}/\text{cm}$ )	0.48	1.00													
TA (mg/L)	0.89	0.57	1.00												
TH (mg/L)	-0.79	-0.08	-0.75	1.00											
Ca <sup>2+</sup> (mg/L)	-0.81	-0.26	-0.69	0.89	1.00										
Mg <sup>2+</sup> (mg/L)	-0.41	0.23	-0.51	0.73	0.34	1.00									
Na <sup>+</sup> (mg/L)	0.85	0.74	0.90	-0.72	-0.77	-0.32	1.00								
Fe <sup>2+</sup> (mg/L)	0.31	0.15	0.36	-0.37	-0.37	-0.20	0.25	1.00							
K <sup>+</sup> (mg/L)	0.11	0.17	0.13	-0.14	-0.14	-0.08	0.10	0.84	1.00						
HCO <sub>3</sub> <sup>-</sup> (mg/L)	0.89	0.57	1.00	-0.75	-0.70	-0.51	0.90	0.36	0.13	1.00					
Cl <sup>-</sup> (mg/L)	-0.39	0.48	-0.40	0.73	0.42	0.88	-0.17	-0.14	0.10	-0.40	1.00				
SO <sub>4</sub> <sup>2-</sup> (mg/L)	0.41	0.63	0.56	-0.41	-0.33	-0.36	0.75	-0.05	-0.11	0.55	-0.09	1.00			
F <sup>-</sup> (mg/L)	0.68	0.42	0.78	-0.66	-0.67	-0.35	0.73	0.48	0.02	0.78	-0.35	0.45	1.00		
SiO <sub>2</sub> (mg/L)	0.18	0.11	0.12	-0.07	-0.34	0.38	0.14	-0.02	-0.34	0.12	0.12	-0.21	0.46	1.00	

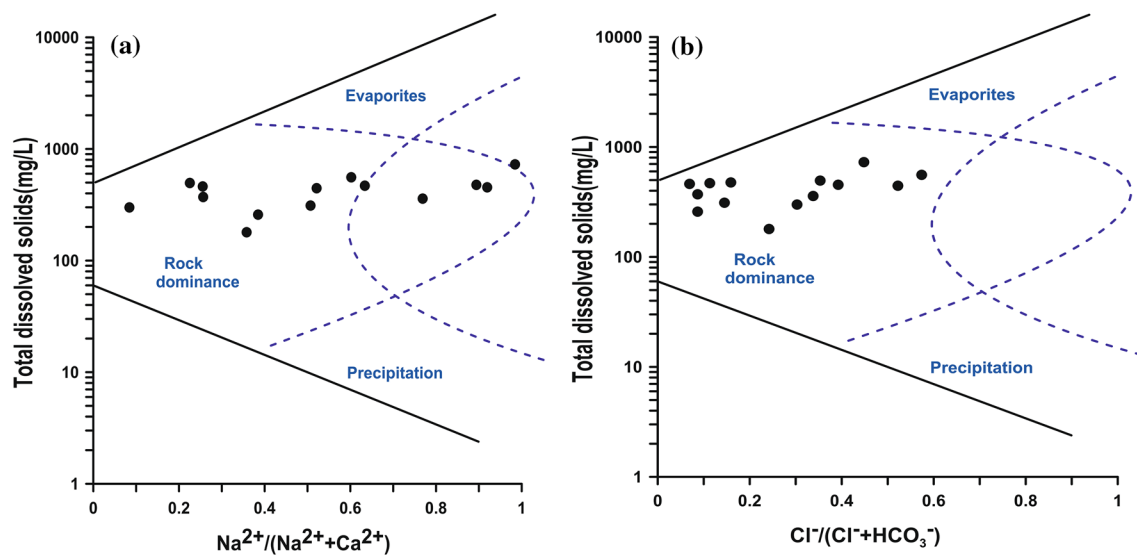


Fig. 4 a Gibbs plot for cations. b Gibbs plot for anions

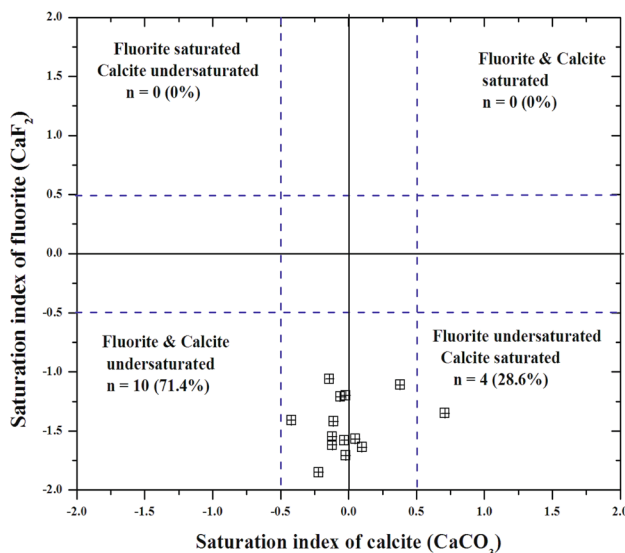


Fig. 5 Plot showing saturation indices of fluorite and calcite

(6.14–7.62), respectively. A major portion of the Arang block is occupied with moderate to unsafe contaminated zones with an area of 768.03 km<sup>2</sup> (84.79% of the total area) whereas safe zones occupy an area of 137.76 km<sup>2</sup> (15.21% of the total area). Unsafe zone is mainly observed in the western portion of the study area underlain by limestone aquifer of Chandi Formation and laterite aquifer whereas; it spreads over the Charmuria limestone and alluvium deposit in the south-eastern portion. Moreover, output map reveals that, the existence of favorable hydro-geomorphological condition such as pediment, buried pediment, flood plain, shallow water table depth (< 8 m) and relatively higher rainfall also contributing to the groundwater contamination. The existence of agricultural

land and rural built-up area are the major land use patterns encountered in the unsafe zone. Agricultural activities in the study area may be one of the major anthropogenic sources contributing to high fluoride and nitrate contamination of groundwater. Presence of sandy loam, gravelly sand clay loam and sandy clay loam also promotes the leaching of surface contamination to the groundwater storage.

### Validation of potential anthropogenic contamination zone map

Three methods are employed for validating the proposed potential anthropogenic contamination zone map, are as follows:

#### Overlying of nitrate and fluoride points

To check the accuracy and reliability of the final output map, initially the reported fluoride contaminated data (fluoride concentration) obtained from NRDWP, Raipur was used. A total number of 11 groundwater fluoride affected wells are superimposed on the PACZ map (Fig. 6b) and a gross precision of 82% in agreement was achieved (Supplementary Table 1). Similarly, 55 wells of measured nitrate concentration are layered on the PACZ map (Fig. 6b) which makes an agreement of 94% (Supplementary Table 2).

#### Similarity analysis for nitrate and fluoride concentrations with respect to PACZ indices

The similarity analysis has been carried out by performing the Pearson's correlation analysis for both nitrate and

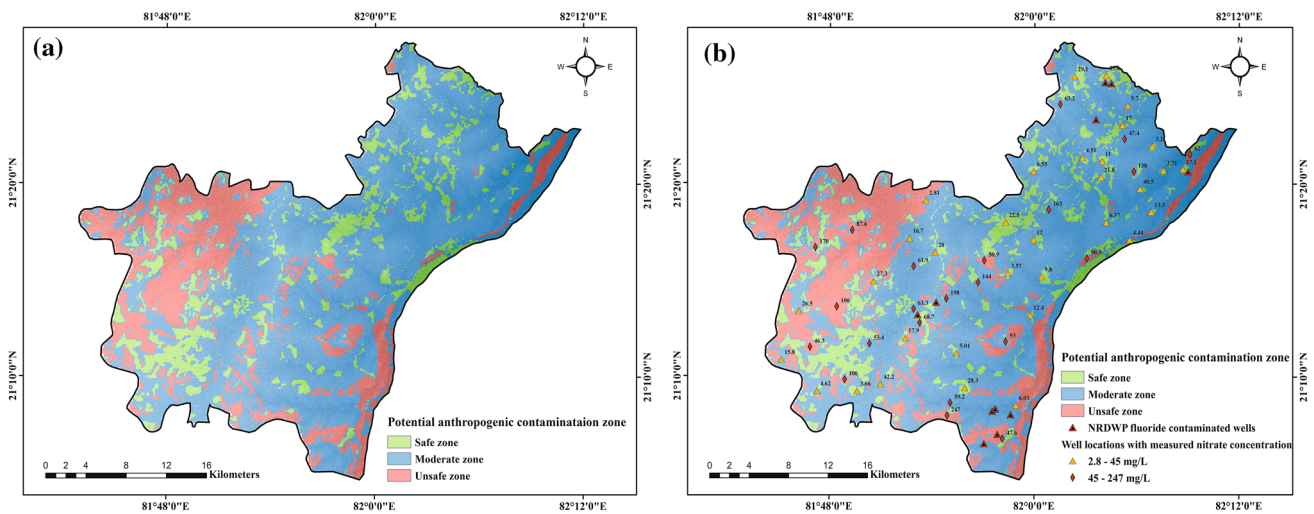


**Fig. 6** **a** Potential anthropogenic contamination zone map of the study area. **b** Model validation—PACZ map with NRDWP reported data of fluoride concentration and measured data of nitrate concentration

fluoride concentration with the potential anthropogenic contamination indices, which shows  $r = 0.62$  and  $r = 0.67$ , respectively (Fig. 7a, b). Hence, nitrate and fluoride concentration data satisfactorily validate the PACZ map.

**Comparison analysis of nitrate and fluoride concentrations with respect to land use patterns**

Nitrate and fluoride concentration wells are further superimposed on the Lulc map of the study area (Fig. 8a) and it shows that all the fluoride contaminated wells fall in agricultural land, whereas for nitrate concentration, out of 55 wells location total 28 numbers of high nitrate contaminated wells are falling in agricultural land, 23 and 4 wells are

concentrated in rural built-up area and waste land, respectively. Furthermore, the mean nitrate concentrations in each land use pattern were computed and the mean nitrate concentrations follow a decreasing trend in the following manner: i.e., agricultural land (mean  $\text{NO}_3 = 75.4 \text{ mg/L}$ ) > rural built-up area (mean  $\text{NO}_3 = 21.8 \text{ mg/L}$ ) > waste land (mean  $\text{NO}_3 = 12.4 \text{ mg/L}$ ) (Fig. 8b). The model validation results obtained by three methods significantly justify the assigned weights and ratings to the various litho-hydrogeological inputs for developing the PACZ model. Therefore, results also support the employed MCDA-AHP technique for computing the normalized weights for the model parameters.

Application of AHP in GIS-based model with various lithological and hydrogeological data can provide a very

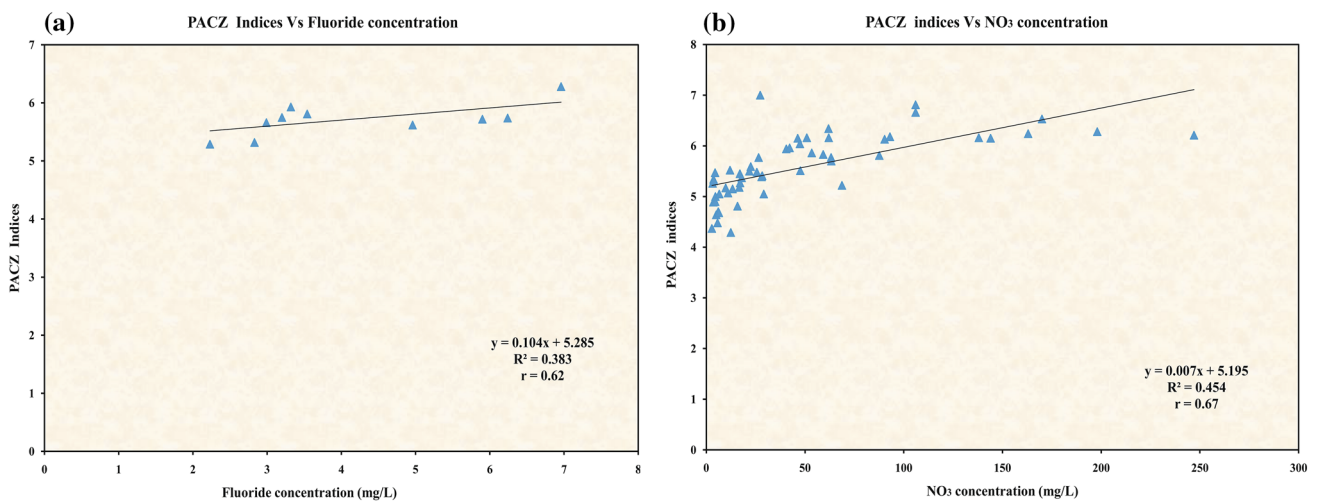


**Fig. 7** Correlation plot: **a** fluoride concentration with model indices, **b** nitrate concentration with model indices

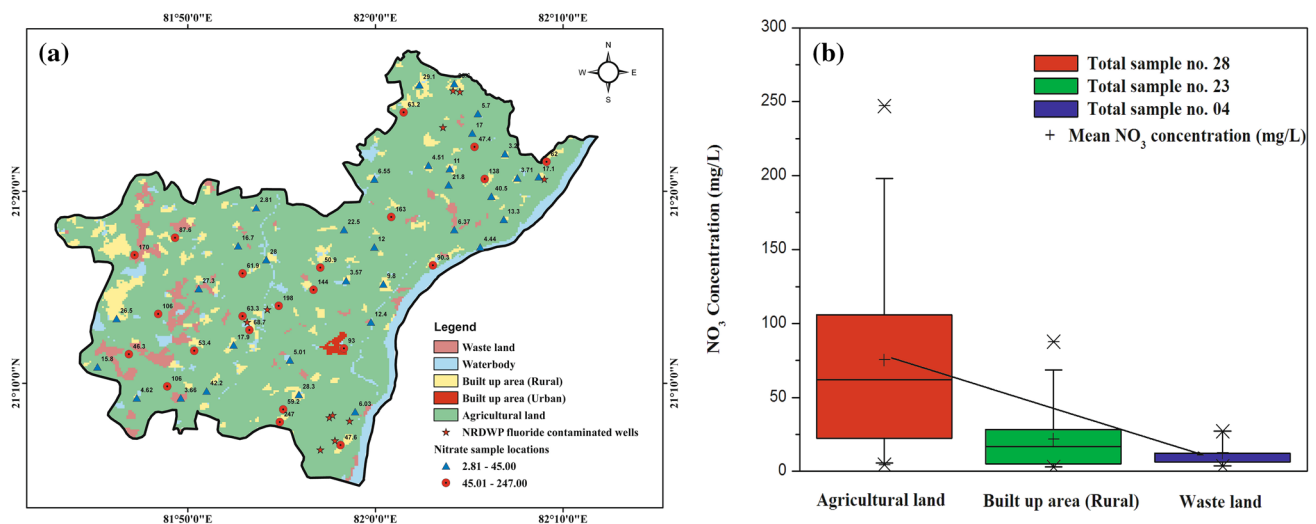


**Fig. 8** a Comparison of Lulc map with fluoride and nitrate concentration. b Box plot of mean nitrate concentration with land use pattern

logical interpretation to groundwater anthropogenic contamination. Various research works were carried out for delineating the anthropogenic potential zone using hydro-geochemical datasets. However, very few studies have been conducted for the same purpose using different litho-hydrogeological data. The present work focused on both litho-hydrogeological and hydro-geochemical study for assessing the groundwater anthropogenic pollution in the study area. The final PACZ map helps to identify the areas of potential fluoride and nitrate contamination and the hydrochemical analysis highlights the significant reason behind the groundwater anthropogenic contamination in the study area. Hence, the prepared final output map can aid planners, designers, engineers as well as the decision-makers of groundwater resource management for proper planning of preventive measures to reduce contamination and also for judicious use of the precious natural resource.

## Conclusions

In the current research study, a GIS–AHP-based litho-hydrogeological approach was developed for Arang Block, Raipur, Chhattisgarh, Central India. A total of ten litho-hydrogeological parameters including geology and aquifer, Lulc, depth to water table, soil type, rainfall distribution, geomorphology, drainage density, slope, elevation and lineament density are considered for MCDA-AHP analysis. The key findings of the present study are presented below:

- Selected parameters were assigned weights based on their relative importance towards delineation of groundwater anthropogenic contamination zones. Weight normalization using MCDA-AHP technique integrated with GIS

platform was performed to obtain a more realistic output of the model.

- Proposed model output revealed that 768.06 km<sup>2</sup> of the total area falls within the moderate to unsafe zone category and rest 137.76 km<sup>2</sup> comes under safe zone category.
- Groundwater physico-chemical data for pH, EC, TA, TH, Ca<sup>2+</sup>, Mg<sup>2+</sup>, Na<sup>+</sup>, Fe<sup>2+</sup>, K<sup>+</sup>, HCO<sub>3</sub><sup>-</sup>, Cl<sup>-</sup>, SO<sub>4</sub><sup>2-</sup>, F<sup>-</sup>, and SiO<sub>2</sub> were selected to perform statistical analysis of groundwater geochemistry. The results of the statistical analysis show that mean pH level in the study area is alkaline in nature (7.62) and the presence of major cations and anions follow the mean increasing trend; K<sup>+</sup> < Mg<sup>2+</sup> < Ca<sup>2+</sup> < Na<sup>+</sup> and F<sup>-</sup> < SO<sub>4</sub><sup>2-</sup> < Cl<sup>-</sup> < HCO<sub>3</sub><sup>-</sup>, respectively.
- Hydro-geochemistry of the groundwater represented by Gibbs's plot shows that rock-water interaction influences the groundwater chemistry. Moreover, the SI value of the calcite mineral (i.e., SI = -0.5 to 0.5) indicates the existence of equilibrium conditions that favored to deficit Ca<sup>2+</sup> concentration in groundwater than the Na<sup>+</sup>, besides ion exchange process (i.e., replacement of Ca<sup>2+</sup> by Na<sup>+</sup>). Whereas, the lack of fluoride-bearing minerals in the aquifer system is responsible for the undersaturated condition of fluorite. However, groundwater fluoride contamination reported in the study area in a disseminated manner, is principally attributed to the non-point anthropogenic sources.
- Finally, to check the reliability and accuracy of the proposed model, NRDWP reported data of fluoride concentration for 11 locations and measured nitrate concentration of 55 locations were superimposed over the resulted PACZ map, which satisfied 82% and 94% of the proposed model. In addition, Pearson's correlation coefficient (*r*)



of 0.62 and 0.67 were achieved between fluoride and nitrate concentration with PACZ model indices. Hence, the results validate the model successfully.

- The proposed concept is implemented in the flat terrain of Raipur district where aquifers are contaminated by elevated fluoride (dispersed manner at places) and nitrate contents due to intensive agricultural practices. Anthropogenic sources such as excessive use of phosphates and nitrogenous fertilizers in agricultural activities are significantly contributing to fluoride and nitrate concentration in groundwater of the current study area, apart from that of emission of fluoride from small scale brick kiln units.

**Acknowledgements** The authors would like to acknowledge the support received from Director IIT (ISM), Departments of Civil Engineering, Chemical Engineering and Applied Geology, IIT (ISM) Dhanbad, during research work. We sincerely acknowledge the editor and anonymous reviewers for improving the quality of the manuscript with their insightful comments. The authors would like to sincerely thank and gratefully acknowledge organizations located in Raipur like CGWB, State Data Centre, and CHIPS for providing the required data and information utilized in the present work. Particularly, the first author/SS is grateful to Mr. Harish Sinha, CHIPS, Raipur, for providing some information/data.

## References

- Ahada CP, Suthar S (2018) Groundwater nitrate contamination and associated human health risk assessment in southern districts of Punjab. *India Environ Sci Pollut Res* 25:25336–25347. <https://doi.org/10.1007/s11356-018-2581-2>
- Akinlalu AA, Adegbuyiro A, Adiat KA, Akeredolu BE, Lateef WY (2017) Application of multi-criteria decision analysis in prediction of groundwater resources potential: a case of Oke-Ana, Ilesa Area Southwestern, Nigeria. *NRIAG J Astron Geophys* 6:184–200. <https://doi.org/10.1016/j.nrjag.2017.03.001>
- Al-Abadi AM, Al-Shamma'a AM, Aljabbari MH (2017) A GIS-based DRASTIC model for assessing intrinsic groundwater vulnerability in northeastern Missan governorate, southern Iraq. *Appl Water Sci* 7:89–101. <https://doi.org/10.1007/s13201-014-0221-7>
- Alabdula'aly AI, Al-Rehaili AM, Al-Zarah AI, Khan MA (2010) Assessment of nitrate concentration in groundwater in Saudi Arabia. *Environ Monit Assess* 16:1–9. <https://doi.org/10.1007/s10661008-0722-7>
- Alonso JA, Lamata MT (2006) Consistency in the analytic hierarchy process: a new approach. *Int J Uncertainty Fuzziness Knowledge Based Syst* 14:445–459. <https://doi.org/10.1142/S0218488506004114>
- Al-shabeeb AR (2016) The use of AHP within GIS in selecting potential sites for water harvesting sites in the Azraq Basin—Jordan. *J Geogr Inf Syst* 8:73. <https://doi.org/10.4236/jgis.2016.81008>
- Amalraj A, Pius A (2013) Health risk from fluoride exposure of a population in selected areas of Tamil Nadu South India. *Food Sci Hum Wellness* 2:75–86. <https://doi.org/10.1016/j.fshw.2013.03.005>
- Appelo C, Postma D (2005) *Geochemistry, groundwater and pollution*. 2nd edn. A.A. Balkema Publishers, Netherlands
- Avtar R, Singh C, Shashtri S, Singh A, Mukherjee S (2010) Identification and analysis of groundwater potential zones in Ken-Betwa river linking area using remote sensing and geographic information system. *Geocarto Int* 25:379–396. <https://doi.org/10.1080/10106041003731318>
- Ayoub S, Gupta AK (2006) Fluoride in drinking water: a review on the status and stress effects. *Crit Rev Env Sci Technol* 36:433–487. <https://doi.org/10.1080/10643380600678112>
- BIS (2012) (Bureau of Indian Standards) IS: 10500 Indian Standards for Drinking Water—Specification. Second revision, New Delhi
- Bonsor HC, MacDonald AM, Davies J (2014) Evidence for extreme variations in the permeability of laterite from a detailed analysis of well behaviour in Nigeria. *Hydrol Process* 28:3563–3573. <https://doi.org/10.1002/hyp.9871>
- Boumans L, Fraters D, van Drecht G (2008) Mapping nitrate leaching to upper groundwater in the sandy regions of The Netherlands, using conceptual knowledge. *Environ Monit Assess* 137:243–249. <https://doi.org/10.1007/s10661-007-9756-5>
- CGWB (2011) Central Ground Water Board, Ministry of water resources, Government of India. Groundwater exploration in Chhattisgarh state, pp. 114–120
- CGWB (2013) Central Groundwater Board, Ministry of water resources, Government of India. Groundwater Brochure of Raipur District, Chhattisgarh, pp. 10
- CGWB (2014) Central Groundwater Board, State report on hydrogeology of Chhattisgarh. North Central Chhattisgarh Region, Raipur, pp. 75
- Chaudhary B, Kumar S (2018) Identification of groundwater potential zones using remote sensing and GIS of KJ Watershed, India. *J Geol Soc India* 91:717–721. <https://doi.org/10.1007/s12594018-0929-3>
- Chidambaram S, Karmegam U, Sasidhar P, Prasanna MV, Manivannan R, Arunachalam S, Anandhan P (2011) Significance of saturation index of certain clay minerals in shallow coastal groundwater, in and around Kalpakkam, Tamil Nadu, India. *J Earth Syst Sci* 120:897–909. <https://doi.org/10.1007/s12040-011-0105-2>
- Craig L, Stillings LL, Decker DL, Thomas JM (2015) Comparing activated alumina with indigenous laterite and bauxite as potential sorbents for removing fluoride from drinking water in Ghana. *Appl Geochem* 56:50–66. <https://doi.org/10.1016/j.apgeochem.2015.02.004>
- Dartan G, Taspinar F (2017) Analysis of fluoride pollution from fertilizer industry and phosphogypsum piles in agricultural area. *J Ind Pollut Control* 33:662–669
- Das S, Gupta A, Ghosh S (2017) Exploring groundwater potential zones using MIF technique in semi arid region: a case study of Hingoli district, Maharashtra. *Spatial Inf Res* 25(749):756. <https://doi.org/10.1007/s41324-017-0144-0>
- DSR (2016) (District Survey Report). As per notifications NO. S.O. 141(E), New Delhi, 15th January, Ministry of Environment, Forest and climate change. Directorate of Geology and Mining Mineral Resources Department, Govt. of Chhattisgarh
- Ducci D (2018) An easy-to-use method for assessing nitrate contamination susceptibility in groundwater. *Geofluids*. <https://doi.org/10.1155/2018/1371825>
- Edmunds WM, Smedley PL (2013) Fluoride in natural waters. In: *Essentials of medical geology*. Springer, Dordrecht, pp 311–336. [https://doi.org/10.1007/978-94-007-4375-5\\_13](https://doi.org/10.1007/978-94-007-4375-5_13)
- Elewa HH, Qaddah AA (2011) Groundwater potentiality mapping in the Sinai Peninsula, Egypt, using remote sensing and GIS-watershed-based modeling. *Hydrogeol J* 19:613–628. <https://doi.org/10.1007/s10040-011-0703-8>
- Elfaki T (2010) Determination, source identification and GIS mapping for nitrate concentration in ground water from Bara aquifer, pp. 12
- Fan AM, Steinberg VE (1996) Health implications of nitrate and nitrite in drinking water: an update on methemoglobinemia occurrence

- and reproductive and developmental toxicity. *Regul Toxicol Pharm* 23:35–43. <https://doi.org/10.1006/rtph.1996.000>
- Farooqi A, Masuda H, Kusakabe M, Naseem M, Firdous N (2007) Distribution of highly arsenic and fluoride contaminated groundwater from east Punjab, Pakistan, and the controlling role of anthropogenic pollutants in the natural hydrological cycle. *Geochem J* 41:213–234. <https://doi.org/10.2343/geochemj.41.213>
- Fienen MN, Arshad M (2016) The International scale of the groundwater issue. In: *Integrated Groundwater Management*. Springer, Cham. [https://doi.org/10.1007/978-3-319-23576-9\\_2](https://doi.org/10.1007/978-3-319-23576-9_2)
- Foster SS, Chilton PJ (2003) Groundwater: the processes and global significance of aquifer degradation. *Philos Trans Royal Soc Lond Ser B Biol Sci* 358:1957–1972. <https://doi.org/10.1098/rstb.2003.1380>
- Gateva PD, Argirova MD (2008) High-nitrate levels in drinking water may be a risk factor for thyroid dysfunction in children and pregnant women living in rural Bulgarian areas. *Int J Hyg Environ Health* 211:555–559. <https://doi.org/10.1016/j.ijheh.2007.10.002>
- Gibbs RJ (1970) Mechanisms controlling world water chemistry. *Science* 170:1088–1090. <https://doi.org/10.1126/science.170.3962.1088>
- Gleeson T, Wada Y, Bierkens MF, van Beek LP (2012) Water balance of global aquifers revealed by groundwater footprint. *Nature* 488:197
- Goolsby DA, Battaglin WA, Hooper RP (1997) Sources and transport of nitrogen in the Mississippi River Basin. In: *American Farm Bureau Federation Workshop*. St. Louis, MO, pp. 14–15
- GWYB (2016) Ground water Year Book of Chhattisgarh, 2015–2016, Central Ground Water Board, Ministry of water resources and Ganga rejuvenation, Government of India, pp. 117–131
- Harker PT, Vargas LG (1987) The theory of ratio scale estimation: saaty's analytic hierarchy process. *Manage Sci* 33:1383–1403. <https://doi.org/10.1287/mnsc.33.11.1383>
- Hatefi Ardakani A, Ekhtesasi M (2016) Groundwater potentiality through analytic hierarchy process (AHP) using remote sensing and geographic information system (GIS). *Geopersia* 6:75–88. <https://doi.org/10.22059/JGEOPE.2016.57823>
- Huang T, Ju X, Yang H (2017) Nitrate leaching in a winter wheat-summer maize rotation on a calcareous soil as affected by nitrogen and straw management. *Sci Rep* 7:42247
- Ibrahim-Bathis K, Ahmed S (2016) Geospatial technology for delineating groundwater potential zones in Doddahalla watershed of Chitradurga district, India. *Egypt J Remote Sens Space Sci* 19:223–234. <https://doi.org/10.1016/j.ejrs.2016.06.002>
- Jabal MSA, Abustan I, Rozaimy MR, Al-Najar H (2014) Fluoride enrichment in groundwater of semi arid urban area: Khan Younis City, southern Gaza Strip (Palestine). *J Afr Earth Sci* 100:259–266. <https://doi.org/10.1016/j.jafrearsci.2014.07.002>
- Javadi S, Kavehkar N, Mousavizadeh MH, Mohammadi K (2011a) Modification of DRASTIC model to map groundwater vulnerability to pollution using nitrate measurements in agricultural areas. *J Agr Sci Tech* 13:239–249
- Javadi S, Kavehkar N, Mohammadi K, Khodadadi A, Kahawita R (2011b) Calibrating DRASTIC using field measurements, sensitivity analysis and statistical methods to assess groundwater vulnerability. *Water Int* 36:719–732. <https://doi.org/10.1080/02508060.2011.610921>
- Jenifer MA, Jha MK (2017) Comparison of analytic hierarchy process, catastrophe and entropy techniques for evaluating groundwater prospect of hard-rock aquifer systems. *J Hydrol* 548(605):624. <https://doi.org/10.1016/j.jhydrol.2017.03.023>
- Jha SK, Mishra VK, Sharma DK, Damodaran T (2011) Fluoride in the environment and its metabolism in humans. Springer, New York. *Rev Environ Contam Toxicol* 211:121–142. [https://doi.org/10.1007/978-1-4419-8011-3\\_4](https://doi.org/10.1007/978-1-4419-8011-3_4)
- Jhariya D, Kumar T, Gobinath M, Diwan P, Kishore N (2016) Assessment of groundwater potential zone using remote sensing, GIS and multi criteria decision analysis techniques. *J Geol Soc India* 88:481–492. <https://doi.org/10.1007/s12594-016-0511-9>
- Jordan C, Smith RV (2005) Methods to predict the agricultural contribution to catchment nitrate loads: designation of nitrate vulnerable zones in Northern Ireland. *J Hydrol* 304:316–329. <https://doi.org/10.1016/j.jhydrol.2004.07.037>
- Kazakis N (2018) Delineation of suitable zones for the application of managed aquifer recharge (MAR) in coastal aquifers using quantitative parameters and the analytical hierarchy process. *Water* 10:804. <https://doi.org/10.3390/w10060804>
- Khan R, Jhariya D (2017) Spatial assessment of groundwater quality with special reference to nitrate pollution in Raipur City, Chhattisgarh state, India using geographical information system. *Int J Adv Geosci* 5:6–12
- Khandare HW (2013) Scenario of nitrate contamination in groundwater: its causes and prevention. *Int J Chem Tech Res* 5:1921–1926
- Kumar MD, Shah T (2006) Groundwater pollution and contamination in India: the emerging challenge. IWMITATA Water Policy Program Draft Paper 1:14
- Kumar B, Singh UK, Mukherjee I (2017) Hydrogeological influence on the transport and fate of contaminants in the groundwater, India. *JSM* 2:1009
- Kumar S, Venkatesh AS, Singh R, Udayabhanu G, Saha D (2018) Geochemical signatures and isotopic systematics constraining dynamics of fluoride contamination in groundwater across Jamui district, Indo-Gangetic alluvial plains, India. *Chemosphere* 205:493–505. <https://doi.org/10.1016/j.chemosphere.2018.04.116>
- Kundu MC, Mandal B (2009) Assessment of potential hazards of fluoride contamination in drinking groundwater of an intensively cultivated district in West Bengal, India. *Environ Monit Assess* 152:97. <https://doi.org/10.1007/s10661-008-0299-1>
- Meeussen JC, Scheidegger A, Hiemstra T, van Riemsdijk WH, Borkovec M (1996) Predicting multicomponent adsorption and transport of fluoride at variable pH in a goethite–silica sand system. *Environ Sci Technol* 30:481–488. <https://doi.org/10.1021/es950178z>
- Mehrabi H, Zeinivand H, Hadidi M (2013) Site selection for groundwater artificial recharge in Silakhor Rangelands using GIS technique. *J Rangeland Sci* 2:687–695
- Murasingh S, Jha R (2013) Identification of groundwater potential zones using remote sensing and GIS in a mine area of Odisha
- Nag S, Kundu A (2018) Application of remote sensing, GIS and MCA techniques for delineating groundwater prospect zones in Kashipur block, Purulia district, West Bengal. *Appl Water Sci* 8:38. <https://doi.org/10.1007/s13201-018-0679-9>
- Olaka LA, Wilke FD, Olago DO, Odada EO, Mulch A, Musolf A (2016) Groundwater fluoride enrichment in an active rift setting: Central Kenya Rift case study. *Sci Total Environ* 545:641–653
- Panahi MR, Mousavi SM, Rahimzadegan M (2017) Delineation of groundwater potential zones using remote sensing, GIS, and AHP technique in Tehran-Karaj plain, Iran. *Environ Earth Sci* 76:792. <https://doi.org/10.1007/s12665-017-7126-3>
- Parkhurst DL, Appelo CAJ (1999) User's Guide to PHREEQC (Version 2): A computer program for speciation, batch-reaction, one-dimensional transport, and inverse geochemical calculations. U.S. Geological Survey, Water Resources Investigations Report 99–4259, Washington
- Pinto D, Shrestha S, Babel MS, Ninsawat S (2015) Delineation of groundwater potential zones in the Comoro watershed, Timor Leste using GIS, remote sensing and analytic hierarchy process (AHP) technique. *Appl Water Sci* 7:503–519. <https://doi.org/10.1007/s13201-015-0270-6>
- Rafique T, Naseem S, Ozsvath D, Hussain R, Bhangar MI, Usmani TH (2015) Geochemical controls of high fluoride groundwater

- in Umarmot sub-district, Thar Desert, Pakistan. *Sci Total Environ* 530:271–278. <https://doi.org/10.1016/j.scitotenv.2015.05.038>
- Raj D, Shaji E (2017) Fluoride contamination in groundwater resources of Alleppey, southern India. *Geosci Front* 8:117–124. <https://doi.org/10.1016/j.gsf.2016.01.002>
- Ramteke LP, Sahayam AC, Ghosh A, Rambabu U, Reddy MR, Papat KM, Rebarry B, Kubavat D, Marathe KV, Ghosh PK (2018) Study of fluoride content in some commercial phosphate fertilizers. *J Fluorine Chem* 210:149–155. <https://doi.org/10.1016/j.jfluc hem.2018.03.018>
- Reddy A, Reddy D, Rao P, Prasad KM (2010) Hydrogeochemical characterization of fluoride rich groundwater of Wailpalli watershed, Nalgonda District, Andhra Pradesh, India. *Environ Monit Assess* 171:561–577. <https://doi.org/10.1007/s10661-009-1300-3>
- Roy S, Dass G (2013) Fluoride contamination in drinking water—a review. *Resour Environ* 3:53–58. <https://doi.org/10.5923/j.re.20130303.02>
- Rusydi AF (2018) Correlation between conductivity and total dissolved solid in various type of water: a review. IOP Publishing, Bristol, p 012019
- Saaty TL (1980) The analytic hierarchy process: planning, priority setting, resource allocation. McGraw-Hill International Book Company, New York
- Saaty TL (2004) Fundamentals of the analytic network process—multiple networks with benefits, costs, opportunities and risks. *J Syst Sci Syst Eng* 13:348–379. <https://doi.org/10.1007/s11518-0060171-1>
- Saaty TL (2007) Time dependent decision-making; dynamic priorities in the AHP/ANP: generalizing from points to functions and from real to complex variables. *Math Comput Modell* 46:860–891. <https://doi.org/10.1016/j.mcm.2007.03.028>
- Senanayake I, Dissanayake D, Mayadunna B, Weerasekera W (2016) An approach to delineate groundwater recharge potential sites in Ambalantota, Sri Lanka using GIS techniques. *Geosci Front* 7:115–124. <https://doi.org/10.1016/j.gsf.2015.03.002>
- Sener E, Davraz A (2013) Assessment of groundwater vulnerability based on a modified DRASTIC model, GIS and an analytic hierarchy process (AHP) method: the case of Egirdir Lake basin (Isparta, Turkey). *Hydrogeol J* 21:701–714. <https://doi.org/10.1007/s10040-012-0947-y>
- Singh R, Syed TH, Kumar S, Kumar M, Venkatesh AS (2017a) Hydrogeochemical assessment of surface and groundwater resources of Korba coalfield, Central India: environmental implications. *Arab J Geosci* 10:318. <https://doi.org/10.1007/s12517-017-3098-6>
- Singh R, Venkatesh AS, Syed TH, Reddy AGS, Kumar M, Kurakalva RM (2017b) Assessment of potentially toxic trace elements contamination in groundwater resources of the coal mining area of the Korba Coalfield, Central India. *Environ Earth Sci*. <https://doi.org/10.1007/s12665-017-6899-8>
- Singh R, Venkatesh AS, Syed TH, Surinaidu L, Pasupuleti S, Rai SP, Kumar M (2018) Stable isotope systematics and geochemical signatures constraining groundwater hydraulics in the mining environment of the Korba Coalfield, Central India. *Environ Earth Sci* 77(15):548. <https://doi.org/10.1007/s12665-018-7725-7>
- Singha S, Pasupuleti S, Singha S, Villuri VGK (2017) An integrated approach for evaluation of groundwater quality in Korba district, Chhattisgarh using Geomatic techniques. *J Environ Biol* 38:865. <https://doi.org/10.22438/jeb/38/5/MRN-600>
- Srivastava SK, Ramanathan AL (2018) Geochemical assessment of fluoride enrichment and nitrate contamination in groundwater in hard-rock aquifer by using graphical and statistical methods. *J Earth Syst Sci* 127:104. <https://doi.org/10.1007/s12040-018-1006-4>
- Thapa R, Gupta S, Guin S, Kaur H (2017) Assessment of groundwater potential zones using multi influencing factor (MIF) and GIS: a case study from Birbhum district, West Bengal. *Appl Water Sci* 7:4117–4131. <https://doi.org/10.1007/s13201-017-0571-z>
- USEPA (2006) Toxicity and Exposure Assessment for Children's Health, 2006
- Vinod PN, Chandramouli PN, Koch M (2015) Estimation of nitrate leaching in groundwater in an agriculturally used area in the state Karnataka, India, using existing model and GIS. *Aquat Procedia* 4:1047–1053. <https://doi.org/10.1016/j.aqpro.2015.02.132>
- Ward M, Jones R, Brender J, de Kok T, Weyer P, Nolan B, Villanueva C, van Breda S (2018) Drinking water nitrate and human health: an updated review. *Int J Environ Res Public Health* 15:1557. <https://doi.org/10.3390/ijerph15071557>
- Wu H, Chen J, Qian H (2016) A modified DRASTIC model for assessing contamination risk of groundwater in the northern suburb of Yinchuan, China. *Environ Earth Sci* 75:483. <https://doi.org/10.1007/s12665-015-5094-z>
- Xiaoyu W, Bin L, Chuanming M (2018) Assessment of groundwater vulnerability by applying the modified DRASTIC model in Beihai City, China. *Environ Sci Pollut Res Res*. <https://doi.org/10.1007/s11356-018-1449-9>
- Yadav A, Sahu YK, Rajhans KP, Sahu PK, Chakradhari S, Sahu BL, Ramteke S, Patel KS (2016) Fluoride contamination of groundwater and skeleton fluorosis in Central India. *J Environ Prot* 7:784. <https://doi.org/10.4236/jep.2016.76071>
- Zhou Z (2015) A global assessment of nitrate contamination in groundwater. International Groundwater Resources Assessment Center, Internship Report

**Publisher's Note** Springer Nature remains neutral with regard to jurisdictional claims in published maps and institutional affiliations.